Photochemical & Photobiological Sciences

Accepted Manuscript

This is an *Accepted Manuscript*, which has been through the Royal Society of Chemistry peer review process and has been accepted for publication.

Accepted Manuscripts are published online shortly after acceptance, before technical editing, formatting and proof reading. Using this free service, authors can make their results available to the community, in citable form, before we publish the edited article. We will replace this *Accepted Manuscript* with the edited and formatted *Advance Article* as soon as it is available.

You can find more information about *Accepted Manuscripts* in the Information for Authors.

Please note that technical editing may introduce minor changes to the text and/or graphics, which may alter content. The journal's standard Terms & Conditions and the Ethical guidelines still apply. In no event shall the Royal Society of Chemistry be held responsible for any errors or omissions in this *Accepted Manuscript* or any consequences arising from the use of any information it contains.

ROYAL SOCIETY OF CHEMISTRY

www.rsc.org/pps

Photochemical & Photobiological Sciences RSCPublishing

COMMUNICATION

Development of Highly Thermoresponsive Fluorescence Sensor Consisting of Plasmonic Silver Nanoprisms and Poly(*N*-isopropylacrylamide)-Fluorophore Composites

Cite this: DOI: 10.1039/xoxxoooooox

Received ooth January 2012,
Accepted ooth January 2012

DOI: 10.1039/xoxxoooooox

www.rsc.org/

Kosuke Sugawa,* Ryutaro Ichikawa, Naoto Takeshima, Yoshimasa Tanoue, Joe Otsuki

We developed a new hybrid consisting of Ag nanoprisms, poly(*N*-isopropylacrylamide) (PNIPAm), and fluorophores via layer-by-layer assembly. The fluorescence intensity below the lower critical solution temperature (LCST) of PNIPAm was 6.4 times stronger than that above the LCST, meaning that the hybrids can function as nanosized highly-thermoresponsive fluorescence sensors.

Introduction

Nanosized fluorescence-based thermometers are expected to emerge as powerful analytical tools in chemistry and biochemistry. Recently, fluorescence thermometers were used for real-time intracellular temperature measurements.[1,2] While various types of thermometers have been developed,[3-7] thermoresponsive fluorescence sensors consisting of fluorophores, thermoresponsive polymers, and metal nanoparticles have been identified to show tremendous potential as new nanosized thermometers. The mechanism of these sensors is suggested to be either energy transfer from photoexcited fluorophores to Au nanospheres[8,9] or fluorescence enhancement of the constituent fluorophores. The enhancement was induced by the generation of local electric fields along with the excitation of the localized surface plasmon resonance (LSPR) of the Ag nanospheres.[10-12] The occurrence of these phenomena largely depends on the distance between the molecules and the metal nanoparticles. Poly(*N*-isopropylacrylamide) (PNIPAm), which undergoes a large volume-phase transition around the lower critical solution temperature (LCST), has been employed as an adjustable spacer between the fluorophores and the surface of the metal nanoparticles.[8-12] However, the resulting sensors were only moderately thermoresponsive with the differences in fluorescence intensity accompanying to the LCST phase transition being less than a factor of four. This is probably because the LSPR band from the Ag nanospheres did not effectively overlap with the bands from the fluorophores. Therefore, we developed a new highly thermoresponsive fluorescence sensor based on triangular Ag nanoplates (Ag nanoprisms: AgPRs) as anisotropic Ag nanoparticles.[13] One of the benefits of employing AgPRs is that the local electric fields generated on AgPRs are much stronger than those generated on normal Ag nanospheres.[14] Therefore, the fluorescence from the fluorophores adjacent to the AgPRs is expected to be significantly enhanced. Another advantage is that the generating wavelength of the LSPR can be tuned from the visible region to the near-infrared region by controlling the aspect ratio (obtained by dividing the edge length by the nanoplate thickness).[13,15] To effectively enhance the fluorescence by LSPR, significant overlapping of the LSPR bands and the absorption and emission bands of the molecules is necessary. Therefore, the use of AgPRs, whose LSPR is tuned to the wavelengths that overlap well with absorption and fluorescence bands of the fluorophores, would be a promising strategy for generating high thermoresponsivity because of the effective fluorescence enhancement.

Materials and methods

2.1 Synthesis of colloidal aqueous solution of PNIPAm-modified AgPRs

A colloidal aqueous solution of Ag nanospheres, which were protected with citric acid, was synthesized using previously reported procedures.[16] In brief, an aqueous solution of $AgNO_3$ (1 mM, 100 mL) was added to an aqueous solution (100 mL) of 0.2 mM of $NaBH_4$ and 5 mM of trisodium citrate under cooling in an ice bath, followed by stirring for 1 h. The average diameter of the resultant silver nanoparticles, which was estimated from their TEM images, was ~10 nm. The pH of the Ag nanosphere solution (5 mL) was adjusted to 11.2 and the solution was irradiated with a 470 nm LED for 12 h,[17] resulting in the formation of a colloidal aqueous solution of the AgPRs protected with citric acid. During this process, the color of the solution changed from yellow to red. Surface modification of AgPRs using PNIPAm was accomplished using a modified version of previously reported methods (Figure 1(A)).[8] Briefly, a 2.0 mg/mL aqueous solution of α-carboxyl ω-terminated PNIPAm (Mw = 37,500; 4mL, Polymer Source) was added to the AgPR solution (2 mL), followed by stirring for 12 h. Centrifugation (14,000 rpm; 20 min) was then repeated three times to remove the excess free PNIPAm and the resultant precipitate was re-dispersed in an equivalent volume of ultrapure water to afford PNIPAm-modified AgPRs.

2.2 Synthesis of colloidal solution of FITC-PNIPAm-modified AgPRs (Figure 1(A))

An aqueous solution of fluorescein isothiocyanate (FITC)-PNIPAm conjugates was prepared by adding 12.8 mM FITC in ethanol/ultrapure water (1/1 v/v, 200 μL) and 4 mg/mL aqueous solution of amino-terminated PNIPAm (Mw = 1000; 1.46 mL, Polymer Source) to 0.1 M carbonate buffer (pH 9.6, 2.5 mL), followed by stirring for 6 h.[8] The conjugate solution (2 mL) was then added to the solution of PNIPAm-modified AgPRs (1 mL), followed by stirring at 20 °C for 2 h. Then, the solution was heated to 30 °C for 2 h and cooled to 20 °C for an additional 2 h under stirring to obtain FITC-PNIPAm-modified AgPR hybrids (FITC/PNIPAm/AgPRs) (Figure 1(A)). Finally, centrifugation was repeated two more times and the resultant precipitate was re-dispersed in an equivalent volume of ultrapure water.

2.3. Measurements:

Absorption and extinction spectra were taken on a JASCO V-630 spectrophotometer. Fluorescence excitation spectra were measured using a JASCO FP-6500 spectrofluorometer. Transmission electron microscope (TEM) images were obtained using a Hitachi HF-2000 system at an acceleration voltage of 200 kV. For negative staining, a solution of 0.1% w/v tungsten acetate in water was placed on a piece of parafilm, and a TEM grid containing the nanoparticles was placed on top of the drop for 1 min. And then the sample was dried using a filter paper and left to dry. Dynamic light scattering (DLS) measurements were carried out at 20 and 40 °C using a Zetasizer Nano ZS (Malvern Instruments Ltd., Malvern, Worcestershire, United Kingdom) at the wavelength of 633 nm.

Results and discussion

The normalized extinction spectra of each colloidal aqueous solution during the synthesis of FITC/PNIPAm/AgPRs are shown in Figure 1(B). As indicated in (a) in the figure, the spectrum of the Ag nanospheres solution showed an LSPR peak at 397 nm, ascribed to a dipole plasmon resonance. After LED irradiation, the peak showed a large red-shift to 494 nm, as seen in (b) in the figure. This would imply photoinduced formation of AgPRs because the peak can be ascribed to the in-plane dipole mode of LSPR.[13,15] The TEM images of the nanoparticles before and after the irradiation are shown in (a) and (b) in Figure 1(C), respectively. While awkward nanospheres with an average diameter of ca. 11 ± 3 nm were formed before irradiation, AgPRs with an average diameter of ca. 28 ± 3 nm were observed after the irradiation. From these results, we confirmed the synthesis of AgPRs by the photoinduction method.

After the PNIPAm modification, the LSPR peak of the AgPRs red-shifted to 519 nm ((c) in Figure 1(B)). It has been reported that the LSPR peak (in-plane dipole mode) from the AgPRs susceptibly red-shifted in response to the increase in the surrounding refractive index due to large surface charge polarizability and increased local electric fields.[18,19] Therefore, this result suggests that the polymer shells, which have a higher refractive index than the surrounding solvent (water), were coated onto the AgPR surfaces.

Following further modification with the FITC-PNIPAm conjugates, negative-stain TEM observation of the hybrids was performed ((c) in Figure 1(C)). The polymer corona was clearly observed around the AgPRs, suggesting that the PNIPAm shells covered the AgPRs. The DLS data (population histogram) for the bare AgPRs showed peaks at around 9 nm and above 100 nm. The

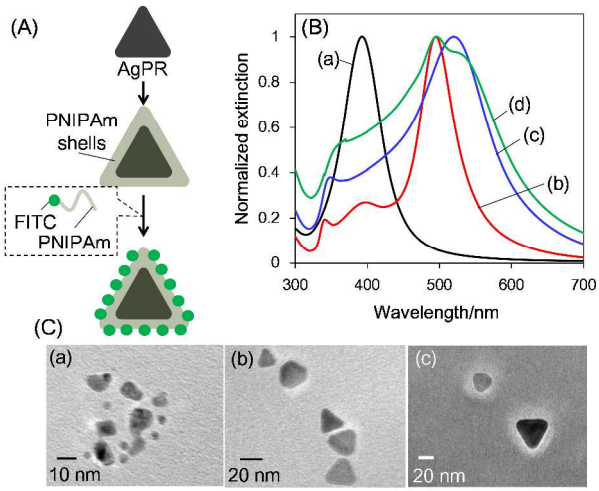

Figure 1 (A) Preparation scheme of FITC/PNIPAm/AgPRs by layer-by-layer assembly. (B) Normalized extinction spectra of the colloidal aqueous solutions of (a) Ag nanospheres, (b) AgPRs, (c) PNIPAm-modified AgPRs, and (d) FITC/PNIPAm/AgPRs (measurement temperature: 25 °C). (C) TEM images of (a) Ag nanospheres, (b) AgPRs, and (c) FITC/PNIPAm/AgPRs negatively stained with tungsten acetate.

data suggest the presence of Ag nanospheres as a seed and AgPRs in solution. After modification with FITC-PNIPAm, the average size got bigger and the size distribution was completely different from that of AgPRs (Figures S1 (b) and (c)). This result indicates that the modification proceeded and bare AgPRs are absent.

The solution of the FITC/PNIPAm/AgPRs hybrids showed a peak at 496 nm with a clear shoulder around 530 nm ((d) in Figure 1(B)). Although the former peak position is coincident with that of the bare AgPRs, the possibility that AgPRs remained in the sample of the FITC/PNIPAm/AgPRs hybrids can be excluded on the basis of the following arguments: (i) DLS measurements showed the absence of bare AgPRs as described above; (ii) TEM observation indicated that most of AgPRs are covered with polymers; and (iii) AgPRs free of citric acids, which were used for the polymer coated AgPRs, would not be stable in solution. Indeed, the hybrids, which were prepared using PNIPAm without FITC, did not show the 496-nm peak (Figure S2). Therefore, the 496-nm absorption peak can be assigned to the FITC. The peak position was slightly red-shifted than that for free FITC in aqueous solution (see Figure 2). The red shift might arise from the formation of intermolecular aggregates and/or differences in microenvironments in the PNIPAm phase. Notably, the LSPR band overlapped well with both the absorption and fluorescence bands of FITC in the hybrid solutions.

In order to investigate the thermoresponsive behavior of the FITC/PNIPAm/AgPRs, we measured the fluorescence spectra of the solution at 40 °C and 20 °C, which were above and below the LCST (30–33 °C) of PNIPAm (Figure 3(A)).[20] At both temperatures, the fluorescence peak derived from FITC was observed at 518 nm. Notably, the fluorescence intensity at 20 °C was *ca.* 6.4 times stronger than that at 40 °C. To check the reproducibility, we prepared five samples of FITC/PANIPAm/AgPRs by the same procedure as above and recorded the ratio of fluorescence intensities at 20 °C and 40 °C. The standard deviation was found to be 3.0. Thus, fluorescence enhancement factor of 6.4 ± 3.0 was established. The fluorescence intensity from FITC remained unchanged when the temperature of an aqueous solution of either free FITC or the FITC-PNIPAm conjugate, without AgPRs, was changed as above (see

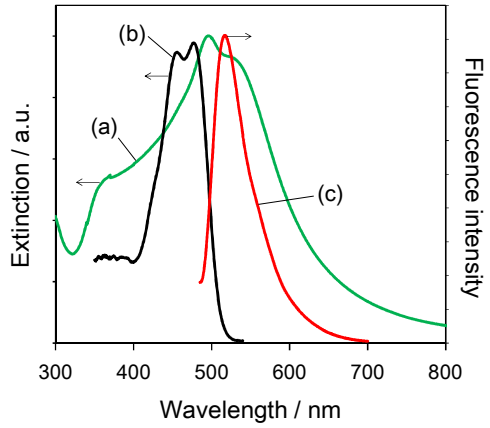

Figure 2 Normalized extinction spectra of (a) colloidal aqueous solutions of FITC/PNIPAm/AgPRs (same as (d) in Figure 1(A)), (b) aqueous solution of 10 μM free FITC. (c) Fluorescence spectrum (λ_{ex} = 490 nm) of the free FITC solution.

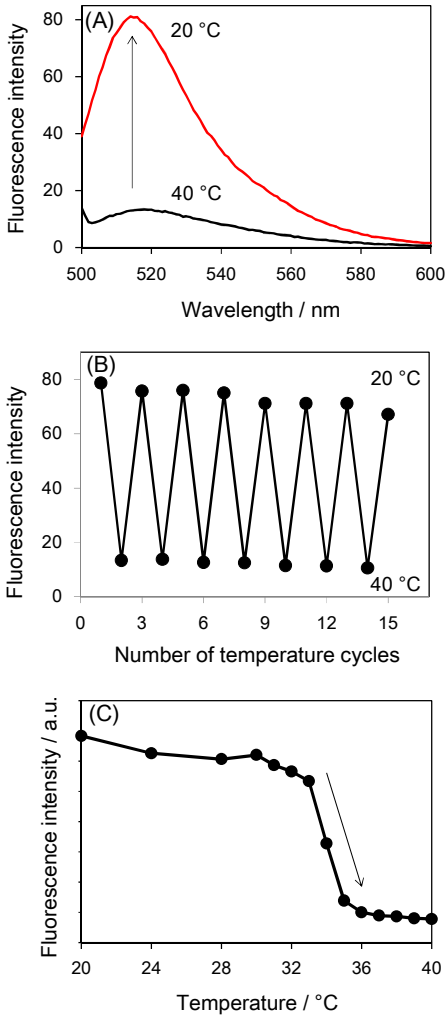

Figure 3 (A) Fluorescence spectra (λ_{ex} = 490 nm) of a solution of FITC/PNIPAm/AgPRs at 20 and 40 °C. (B) Changes in the fluorescence intensities at 518 nm with temperature cycles. (C) Temperature dependence of the FITC/PNIPAm/AgPRs at 518 nm.

Figure S3 and S4). This result indicates that the large change in the fluorescence intensity was due to the formation of FITC/PNIPAm/AgPRs hybrids. In addition, as shown in Figure 3(B), emission/quenching of the hybrids occurred reversibly upon heating and cooling, suggesting that fluorescence switching can be repeated several times without affecting the thermoresponsivity. In order to confirm that the fluorescence switching was driven by the volume-phase transition of PNIPAm shells, the fluorescence spectra of the solution at various temperature points in the range 20–40 °C (Figure 3(C)) were measured. As expected, the fluorescence decreased remarkably in the range 32–36 °C, corresponding to the LCST of PNIPAm. These results clearly indicate that the large fluorescence switching was due to the thermoresponsivity of PNIPAm.

The fluorescence intensity ratios below and above the LCST for previously reported metal nanoparticle-based thermoresponsive sensors range within 1.4–3.7.[8-12] On the other hand, the ratio obtained in the current study was 6.4, signifying that our metal nanoparticle-based fluorescence sensors show higher thermoresponsivity. The large fluorescence change is possibly due to two factors that may lead to the effective enhancement and/or quenching of the fluorescence from FITC. One factor is that the main LSPR band from the AgPRs overlapped well with both the absorption and fluorescence bands of FITC, as shown in Figure 2. When the distance between the fluorophores and the surfaces of the plasmonic silver nanospheres exceeds 1–4 nm, depending on the nanosphere size, the substantial overlap of the LSPR band with both the absorption and emission bands of the fluorophores can lead to a strong enhancement of the fluorescence because of the synergistic effect of photoexcitation enhancement and increased radiative decay rate.[21,22] Conversely, when the aforesaid distance is below 1–4 nm, the quenching will be dominant because the quenching via nonradiative Förster-like energy transfer and/or electron transfer predominates over the fluorescence enhancement.[22,23] Therefore, we suggest that the drastic change in fluorescence intensity around the LCST is partly due to the changes in the distance between the AgPR surfaces and FITC. Below the LCST, the PNIPAm polymer chains would take more extended conformation resulting in larger AgPR-FITC distances, while, above the LCST, the polymer would be more compact resulting in closer AgPR-FITC distances. The other factor that may cause the fluorescence changes is the change in aggregation states of the dyes below and above the LCST, as described in the literature.[9] The DLS analysis showed that the average size measured at 40 °C was fairly larger (658 nm) than that at 20 °C (231 nm) (see Figure S1). This result suggests that the aggregation of the hybrids, which can lead that may facilitate dye aggregation within the hybrids leading to the dye quenching of FITC, occurred above the LCST.[9] Combined contributions of these two factors, i.e., changes in the dye-AgPRs distances and changes in the aggregation states of the dyes, may effect the fluorescence on/off effect. Particularly, the good overlap of the LSPR band of AgPRs and the absorption and fluorescence bands of FITC is considered beneficial in the large on/off ratio achieved in this study.

Conclusion

A new nanosized, highly thermoresponsive sensor utilizing Ag nanoprisms has been developed. These nanoprisms can tune the generating wavelength of the LSPR band and are expected to generate strong local electric fields. To clarify the detailed mechanisms of the sensors and further improve the thermoresponsivity, future investigations should address the effects of the distance between the fluorophores and the Ag nanoprisms on the fluorescence enhancement and fluorescence quenching of the fluorophores.

Acknowledgements

The authors thank Prof. T. Hayashita, Dr. T. Hashimoto, Dr. Y. Tsuchido and H. Kobayashi (Sophia University) for DLS measurement.

Notes and references

College of Science and Technology, Nihon University, Chiyoda, Tokyo 101-8308, Japan

1 K. Okabe, N. Inada, C. Gota, Y. Harada, T. Funatsu, S. Uchiyama, Intracellular temperature mapping with a fluorescent polymeric thermometer and fluorescence lifetime imaging microscopy, *Nat. Commun.*, 2013, **3**, 1714/1-9.

2 Y. Takei, S. Arai, A. Murata, M. Takabayashi, K. Oyama, S. Ishiwata, S. Takeoka, M. Suzuki, A nanoparticle-based ratiometric and self-calibrated fluorescent thermometer for single living cells, *ACS Nano*, 2014, **8**, 198-206.

3 N. Chandrasekharan, L. A. Kelly, A dual fluorescence temperature sensor based on perylene/exciplex interconversion, *J. Am. Chem. Soc.*, 2001, **123**, 9898-9899.

4 S. Uchiyama, Y. Matsumura, A. Prasanna de Silva, K. Iwai, Fluorescent molecular thermometers based on polymers showing temperature-induced phase transitions and labeled with polarity-responsive benzofurazans, *Anal. Chem.*, 2003, **75**, 5926-5935.

5 C. Gota, K. Okabe, T. Funatsu, Y. Harada, S. Uchiyama, Hydrophilic fluorescent nanogel thermometer for intracellular thermometry, *J. Am. Chem. Soc.*, 2009, **131**, 2766-2767.

6 T. Tsuji, S. Yoshida, A. Yoshida, S. Uchiyama, Cationic fluorescent polymeric thermometers with the ability to enter yeast and mammalian cells for practical intracellular temperature measurements, *Anal. Chem.*, 2013, **85**, 9815-23.

7 R. E. Brewster, M. J. Kidd, M. D. Schuh, Optical thermometer based on the stability of a phosphorescent 6-bromo-2-naphthol/a-cyclodextrin2 ternary complex, *Chem. Commun.*, 2001, 1134-1135.

8 J. Wongkongkatep, R. Ladadat, W. Lappermpunsap, P. Wongkongkatep, P. Phinyocheep, A. Ojida, I. Hamachi, Thermoresponsive fluorescent sensor based on core/shell nanocomposite composed of gold nanoparticles and poly(N-isopropylacrylamide), *Chem. Lett.*, 2010, **39**, 184-185.

9 A. Nagai, R. Yoshii, T. Otsuka, K. Kokado, Y. Chujo, BODIPY-based chain transfer agent: reversibly thermoswitchable luminescent gold nanoparticle stabilized by BODIPY-terminated water-soluble polymer, *Langmuir*, 2010, **26**, 15644-15649.

10 J. Liu, A. Li, J. Tang, R. Wang, N. Konga, T. P. Davis, Thermoresponsive silver/polymer nanohybrids with switchable metal enhanced fluorescence, *Chem. Commun.*, 2012, **48**, 4680-4682.

11 F. Tang, N. Ma, L. Tong, F. He, L. Li, Control of metal-enhanced fluorescence with pH- and thermoresponsive hybrid microgels, *Langmuir*, 2012, **28**, 883-888.

12 F. Tang, N. Ma, X. Wang, F. He, L. Li, Hybrid conjugated polymer-Ag@PNIPAM fluorescent nanoparticles with metal-enhanced fluorescence, *J. Mater. Chem.*, 2011, **21**, 16943-16948.

13 R. Jin, Y. Cao, C. A. Mirkin, K. L. Kelly, G. C. Schatz, J. G. Zheng, Photoinduced conversion of silver nanospheres to nanoprisms, *Science*, 2001, **294**, 1901-1903.

14 E. Hao, G. C. Schatz, Electromagnetic fields around silver nanoparticles and dimers, *J. Chem. Phys.*, 2004, **120**, 357-366.

15 R. Jin, Y. C. Cao, E. Hao, G. S. Métraux, G. C. Schatz, C. A. Mirkin, Controlling anisotropic nanoparticle growth through plasmon excitation, *Nature*, 2003, **425**, 487-90.

16 K. Sugawa, Y. Tanoue, Simple fabrication of two-dimensional self-assemblies consisting of gold and silver nanoparticles at an air/toluene interface and their surface-enhanced raman scattering activity, *Jpn. J. Appl. Phys.*, 2012, **51**, 06FG10.

17 K. G. Stamplecoskie, J. C. Scaiano, Light emitting diode irradiation can control the morphology and optical properties of silver nanoparticles, *J. Am. Chem. Soc.*, 2010, **132**, 1825-1827.

18 D. E. Charles, D. Aherne, M. Gara, D. M. Ledwith, Y. K. Gun'ko, J. M. Kelly, W. J. Blau, M. E. Brennan-Fournet, Versatile solution phase triangular silver nanoplates for highly sensitive plasmon resonance sensing, *ACS Nano*, 2010, **4**, 55-64.

19 K. M. Mayer, J. H. Hafner, Localized Surface Plasmon Resonance Sensors. *Chem. Rev.*, 2011, **111**, 3828-3857.

20 R. Pelto, Temperature-sensitive aqueous microgels, *Adv. Colloid. Interface. Sci.*, 2000, **85**, 1-33.

21 J. R. Lakowicz, Radiative decay engineering: biophysical and biomedical applications, *Anal. Biochem.*, 2001, **298**, 1-24.

22 D. V. Guzatov, S. V. Vaschenko, V. V. Stankevich, A. Y. Lunevich, Y. F. Glukhov, S. V. Gaponenko, Plasmonic enhancement of molecular fluorescence near silver nanoparticles: theory, modeling, and experiment, *J. Phys. Chem. C*, 2012, **116**, 10723-10733.

23 D. Cheng, Q.-H. Xu, Separation distance dependent fluorescence enhancement of fluorescein isothiocyanate by silver nanoparticles, *Chem. Commun.*, 2007, 248-50.